68th Adv. Beam Dyn. Workshop High-Intensity High-Brightness Hadron Beams HB2023, Geneva, Switzerland JACoW Publishing
ISBN: 978-3-95450-253-0 ISSN: 2673-5571 doi:10.18429/JACoW-HB2023-WEC3I2

MITIGATION OF SPACE CHARGE EFFECTS IN RHIC AND ITS INJECTORS

V. Schoefer*, C. Gardner, K. Hock, H. Huang, C. Liu, K. Zeno
Brookhaven National Laboratory, Upton, NY, USA

Abstract

The RHIC collider physics programs, in particular its polarized proton and low energy heavy ion components, present unique challenges for maintaining collider performance in the presence of space charge effects. Polarized beam performance is especially sensitive to emittance increases, since they decrease both the luminosity and polarization. Operation of the collider with gold beams at sub-injection energies (down to 3.85 GeV/n Au) with space charge tune shifts up to 0.1 required special care to optimize both the ion lifetime and its interaction with the electron-beam cooler. We describe the operational experience in these modes and some of the mitigation efforts.

INTRODUCTION

The Relativistic Heavy Ion Collider and its injectors (Fig. 1) provide collisions of a wide range of nuclei for two main physics programs. The heavy ion program is aimed at studying the properties of the quark-gluon plasma. In particular, during operation from 2019-2021, the collider was operated with gold beam in a range of beam energies from 3.85 to 9.8 GeV/n, well below the design collision energy of 100 GeV/n (in fact at or below the nominal injection energy of 9.8 GeV/n). The goal of this measurement campaign (called Beam Energy Scan II or BES-II) was to explore center-of-masss collision energies in the range of the QCD critical point [1–3]. The second physics program consists of polarized proton collisions at beam energies of 100 and 255 GeV, which explores the origin and composition of the spin of the proton constituents [4]. While neither the heavy ion nor the polarized proton program are "intensity frontier" accelerator programs, their particular needs nevertheless require special care to mitigate the effects of space charge on collider performance.

For polarized beams, the figure of merit for collider operation with polarized beams is either LP^2 (for transverse polarization) or LP^4 (for longitudinal polarization) where L is the luminosity and P is the polarization. Since the main depolarizing mechanisms in RHIC and its injectors are intrinsic resonances, the effects of which increase with increasing emittance, any increase in the emittance degrades the figure of merit rapidly, since it decreases both the luminosity and the polarization [5, 6].

For heavy ion beams like gold, reaching the requisite per bunch intensities requires multiple longitudinal bunch merges in both the Booster and AGS. Limitation on the RF cavity frequency ranges require that these merges happen at

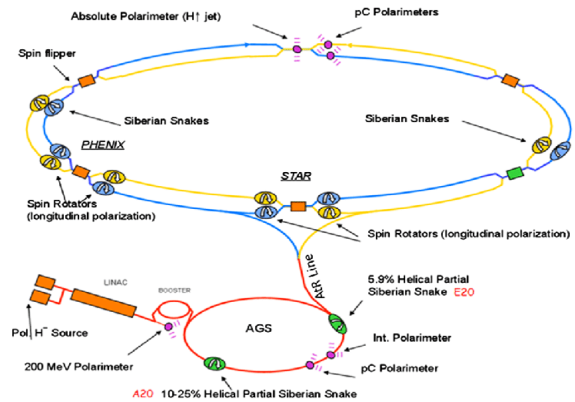

Figure 1: RHIC complex.

relatively low energies, resulting in large space charge tune shifts and ensuing beam loss (e.g., [1, 7]).

RHIC low-energy heavy ion operation is a special case. At the nominal RHIC collision energy of 100 GeV/n, space charge effects are generally neglible. Operation for BES-II, however, posed a particular challenge because at the lowest energies, collisions took place with space charge tune shifts of up to 0.1. Low-energy operation also involved ion beam interaction with the electron beam of the Low-Energy RHIC electron Cooler (LEReC), further constraining the optimum configuration [1, 8–10].

In the following we review selected cases and mitigating measures where space charge effects have created bottlenecks to machine performance for both polarized proton and heavy ion operation.

POLARIZED PROTONS

The primary sources of depolarization in the RHIC injector chain are intrinsic resonances. The strengths of these resonance depend on the betatron amplitudes of the particles and are stronger for larger amplitudes. Depolarization due to these resonance results in a transverse polarization profile, where cross sections of the beam distribution with larger betatron amplitudes have lower polarization. Transverse emittance increases result therefore in decreases of both the luminosity and the polarization [5, 11]. The effects of intrinsic resonances are measured using a thin carbon target inserted at different transverse locations in the beam (Fig. 2).

Figure 3 shows typical measured deterioration of the polarization and transverse emittances with intensity at AGS extraction energy, which are well approximated by linear fits (show in the plots). One can use those measured linear dependences to make predictions of the relative change in

* schoefer@bnl.gov

ISBN: 978-3-95450-253-0 ISSN: 2673-5571 doi:10.18429/JACoW-HB2023-WEC3I2

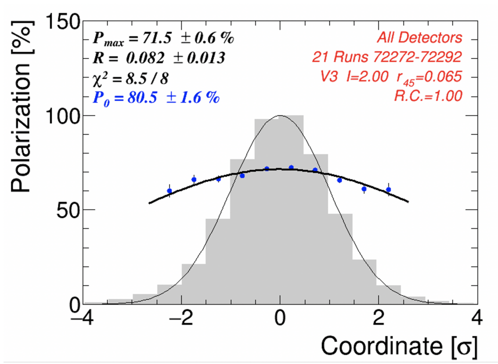

Figure 2: Horizontal polarization profile measured with a thin carbon target at AGS extraction. Intensity profile is shown in gray. The polarization (blue) decreases toward the edges of the intensity profile due to intrinsic depolarizing resonances.

figures of merit (L, LP^2, LP^4) under various assumptions. If emittance and polarization were independent of the intensity, one expects the usual quadratic increase of the luminosity on intensity. However, when the effects of emittance and polarization are included, the benefits of increasing the intensity are dramatically decreased, as shown in Fig. 4. For figure of merit calculations that include the intensity-dependent decrease in polarization, the expected change is closer to linear than quadratic in the intensity.

In the Booster

The polarized proton beam is produced by the OPPIS (Optically Pumped Polarized Ion Source) and accelerated via Linac as an H^- beam to 200 MeV kinetic energy. A 300 µs pulse of H^- is strip injected into the Booster through a carbon foil over 250 turns. The intensity per pulse can be as high as 1×10^{12}, but $6 - 8 \times 10^{11}$ is typical in operation. After the end of the Linac pulse, the circulating beam is pulled off the foil by a fast orbit bump in under 1 ms. The coasting beam is adiabatically captured in the RF and then accelerated (Fig. 5). Later in the acceleration cycle the beam is transversely scraped down by steering into an aperture (primarily vertically) to reduce the intensity to the RHIC requirement of $2 - 3 \times 10^{11}$ by retaining the bright beam core.

Figure 6 shows the tune footprints of the Booster beam just after injection and capture respectively. Injection occurs at a tune near but just above the half-integer (counterintuitively, from a space charge perspective) and then is moved rapidly upward in both planes before bunching begins.

The near half-integer injection tune is motivated by foil scattering considerations. During injection a set of quadrupoles normally used for stop-band correction are used to minimize the beta functions at the foil location, which minimizes emittance growth due to scattering [12–14]. The tune is moved upward away from the half integer before bunching increases the tune shift. The tune setpoint for injection is empirically determined by the trade-off between emittance

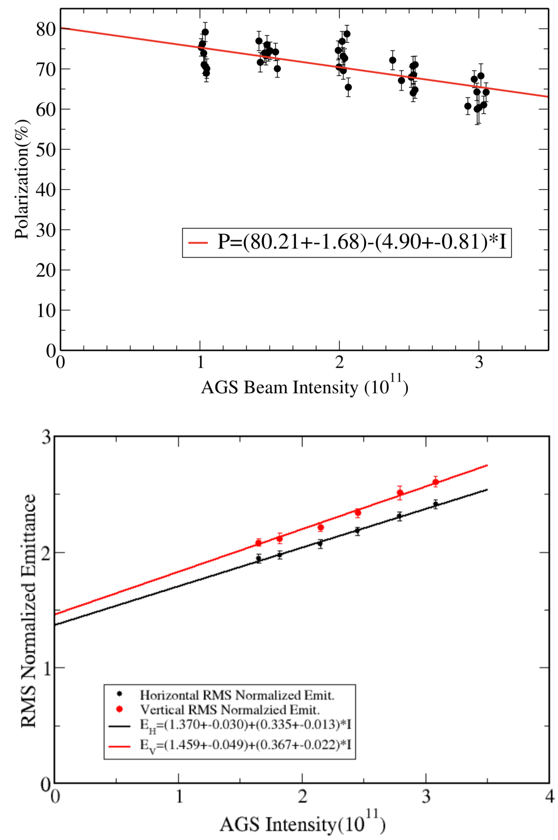

Figure 3: (a) Polarization and (b) transverse emittances as functions of AGS extraction intensity.

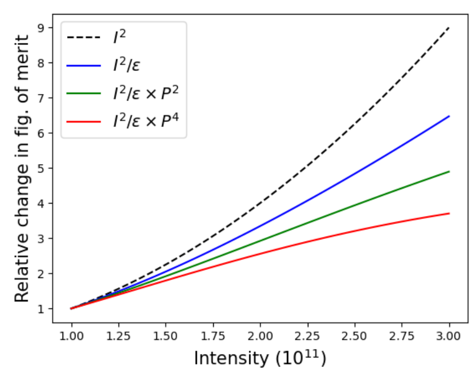

Figure 4: Predicted relative change in polarized collider figures of merit assuming the emittance and polarization are independent of intensity (black), the emittance dependence of Fig. 3(a) (blue) and both the emittance and polarization deterioration of Fig. 3(a,b), for transverse (green) and longitudinal (red) spin physics programs.

ISBN: 978-3-95450-253-0 ISSN: 2673-5571 doi:10.18429/JACoW-HB2023-WEC3I2

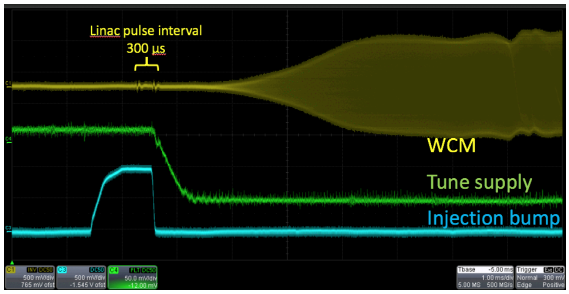

Figure 5: The Booster injection process. As soon as the 300 µs Linac pulse ends, the circulating beam is steered off the injection foil to prevent more scattering. The tunes are raised away from the half-integer before the beam is bunched.

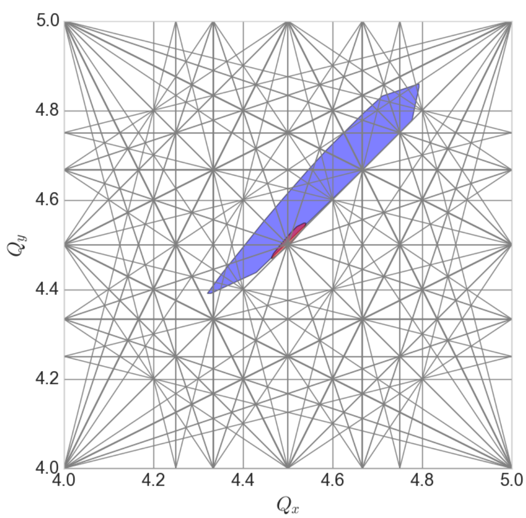

Figure 6: Booster tune footprint (with resonances up to 5th order) from direct space charge for coasting beam just after injection (red) and for bunched beam just after capture into h=1 (blue).

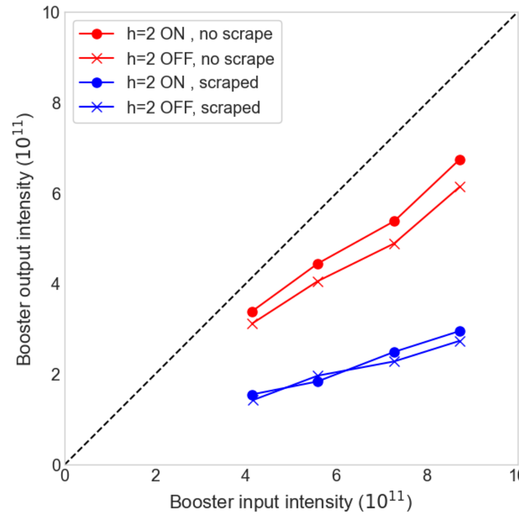

Figure 7: Booster transmission improvement with h=2. Dashed line indicated case of perfect transmission.

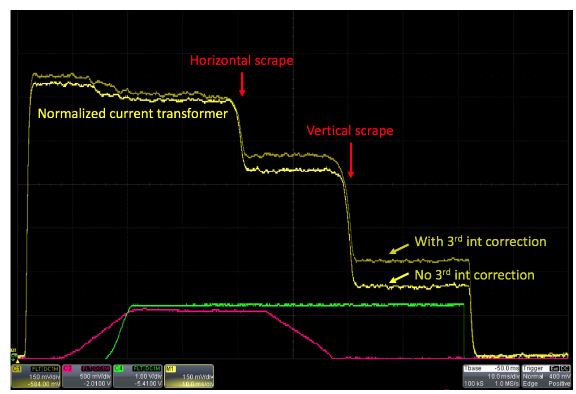

Figure 8: Booster intensity transmission through transverse emittance scraping with and without third integer stopband correction.

increase due to foil scattering and that due to proximity to the half integer.

Proton RF capture in the Booster is typically on harmonic h=1. In 2015 a second harmonic at h=2 was added (using existing RF cavities), out of phase with the main harmonic resulting in a 25 % reduction in the peak current. Because the large amount of transverse scraping introduces a strong correlation between beam emittance and intensity (and because there is no direct measurement of the beam size available in the Booster), the effectiveness of space charge mitigation efforts is often gauged by intensity transmission through the transverse scrapes. Figure 7 shows the improvement of the beam transmission in the presence of the second harmonic. Without scraping, there is increased transmission through the Booster cycle at all intensities. There is a 15 % increase in the transmission to Booster extraction for typical input intensities when fixed amount of scraping is present. The difference in relative intensity gains between the scraped and unscraped cases implies that in the unscraped case, much of the increased intensity is in high amplitude tails, which are not preserved in the scraped case.

Resonance stopband correction using dedicated multipoles has been employed in the Booster since its early days as a high intensity injector to the AGS [15–17]. During high intensity operations $>10^{13}$ protons per pulse were accelerated with a linear space charge tune shift of $\Delta Q_{sc} \approx 0.35$ at injection energy. The stopband correction remains effective at preserving the brightness of the lower intensity (but also lower emittance) polarized proton beam. The improvement to the beam brightness (as measured by increased efficiency through the transverse scrapes) due to third integer stopband correction is shown in Fig. 8.

Polarized Protons in AGS

In general, the strongest depolarizing resonances are associated with the vertical betatron motion. Optimal polarization at AGS extraction is generally achieved when the transvserse scraping in the Booster is more heavily in vertical than horizontal. This results in asymmetric normalized trans-

68th Adv. Beam Dyn. Workshop High-Intensity High-Brightness Hadron Beams HB2023, Geneva, Switzerland JACoW Publishing
ISBN: 978-3-95450-253-0 ISSN: 2673-5571 doi:10.18429/JACoW-HB2023-WEC3I2

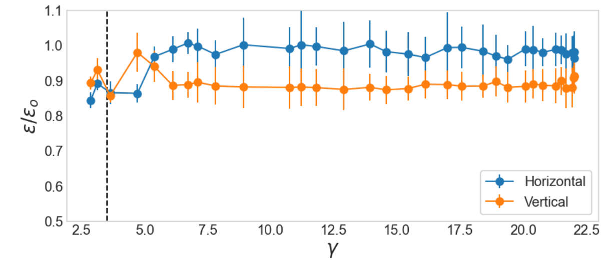

Figure 9: Relative change in transverse emittances in AGS when the peak current is reduced from injection ($\gamma = 2.5$) through $\gamma = 3.5$ (marked with vertical dashed line).

verse emittances $\epsilon_{x,y} \approx 8.4, 3.4\,\mu\text{m}$ and therefore asymmetric space charge tune shifts $\Delta Q_{sc,x,y} = -0.11, -0.23$ [18].

The primary space charge mitigation effort for protons in AGS is a dual harmonic RF defocusing to reduce the peak current in a manner similar to that in the Booster. The main AGS RF acceleration harmonic is h=6, which is augmented by an out of phase voltage at h=12 to flatten the longitudinal distribution, resulting in a 15 % reduction in the peak current.

Two of the ten available AGS RF cavities supply the h=12 voltage. This defocusing voltage is maintained through early acceleration until the acceleration rate approaches its maximum near $\gamma = 3.5$. At that point the large synchronous phase prevents effective bunch flattening and the h=12 cavities are switched back to h=6 in order to provide maximum bucket area during acceleration [18, 19]. At $\gamma = 3.5$ the γ^{-3} energy dependence of the space charge tune shift has already reduced the tune shift to <40 % of its injection value. The reduction in peak current resulted in a 10 % reduction in the vertical transverse emittance that persisted through acceleration, but little change in the horizontal (Fig. 9). This is consistent with a smaller horizontal space charge tune spread due to the larger horizontal emittance.

SPACE CHARGE DURING GOLD OPERATION

AGS

RHIC operation with gold beam requires up to 2.5×10^9 particles per bunch at RHIC injection. This is achieved through a series of longitudinal adiabatic bunch merges in both the Booster and the AGS. The exact scheme depends on which ion source (the Tandem van de Graaf or Electron Beam Ion Source (EBIS)) is being used.

Most recently the primary source has been the EBIS. In this configuration Au ions are injected into the Booster with a total energy of 0.93 GeV/n, captured on harmonic h=4 and accelerated to 1 GeV/n. There a combination of harmonics 1,2 and 4 are used to perform two consecutive 2:1 merges resulting in a single bunch which is accelerated to Booster extraction energy (1.03 GeV/n). Twelve such Booster cycles are transferred to the AGS. There the bunches are merged in two steps from 12 to 6 bunches and then from 6 to 2 using a complex program of voltages at harmonics h=4,8,12 and 24

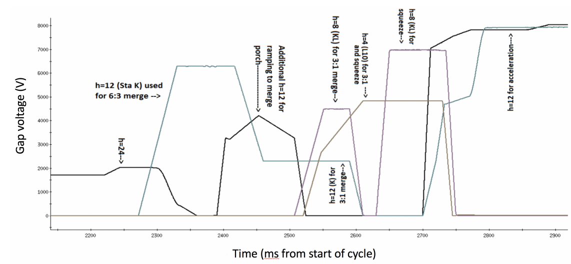

Figure 10: Voltage program for merges for to 6⟶3 and 3⟶1 merges for Au beam in the AGS. As shown there is an acceleration from injection energy ($\gamma = 1.11$) to an intermediate porch ($\gamma = 1.17$) between the first and second merges (2400-2500 ms). The increased energy alleviates the peak space charge forces after the second merge.

(Figs. 10 and 11). In this scheme the space charge bottleneck occurs near the end of the merges when the voltage on the h=12 harmonic is raised in preparation for acceleration [20, 21].

Prior to 2016, the merges in the AGS had been constrained to occur at injection energy by frequency limits on the lower harmonic cavities (h=4,8). For RHIC Run 16, those cavities were modified to allow higher frequency (and therefore a merge at higher energy). Increasing the Booster to AGS transfer energy was not feasible at the time. Instead, a short acceleration stage from $\gamma = 1.11$ to $\gamma = 1.17$ was inserted between the first and second stages of the merge. This reduces the space charge tune shifts by ~15 % and removed the intensity dependent losses. The peak intensity achieved at AGS extraction in this merge/acceleration/merge scheme is 12 % higher than achieved in 2015 with a similar merge scheme, but performed entirely at injection energy [20].

Low-energy RHIC Operation

The principle limitation for high energy heavy ion operation in RHIC is not space charge, but intrabeam scattering, which remains important at the energy and time scales for nominal 100 GeV/n Au operations [22]. The low-energy

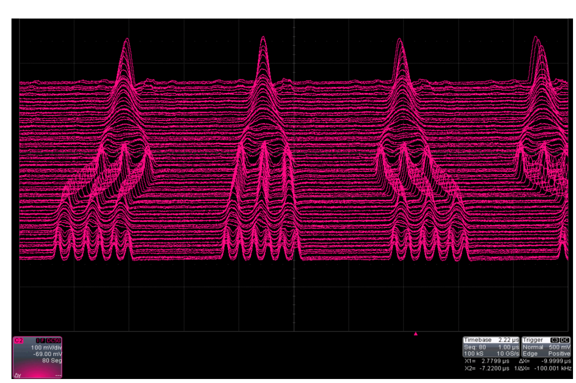

Figure 11: Wall current monitor measurement during the AGS 6⟶3⟶1 merges. (Each trace shows more than one turn).

ISBN: 978-3-95450-253-0 ISSN: 2673-5571 doi:10.18429/JACoW-HB2023-WEC3I2

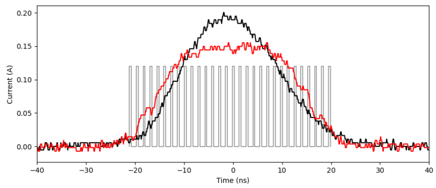

Figure 12: RHIC bunches at 3.85 GeV/n with only a 9 MHz voltage (black) and with 9 MHz plus 28 MHz defocusing voltage (red). The LEReC electron bunch structure (gray) shows the 30 bunches with 704 MHz spacing and 0.4 ns bunch widths.

RHIC program, however, operated in an energy range from 3.85 GeV/n to 9.8 GeV/n. In this energy range, both intra-beam scattering and space charge ($\Delta Q_{sc} \approx 0.11$ at the lowest energy) are important.

The intrabeam scattering limitation on lifetime at or below 9.8 GeV/n was ameliorated by the introduction of the LEReC electron cooler [9]. Optimization of the integrated luminosity at each energy was a complicated, iterative process between both ion and electron beam parameters [1]. The nominal RHIC tunes near 0.23 were favorable to cooling efficiency and minimizing losses driven by the space charge kicks of the electron beam on the ions. Low fractional tunes, near 0.1, were favorable for ion beam lifetime, but increased losses when the ion beam interacted with the space charge kicks of the electron cooler [23]. At the lowest energy, 3.85 GeV/n, a working point of 0.12 was found to be optimal for integrated luminosity, balancing gold beam lifetime with cooling efficiency.

The space charge forces were reduced during the 3.85 GeV/n operation with longitudinal bunch flattening, similar to the injectors. The main storage bucket was provided by 180 kV of 9 MHz voltage. The bunches were then defocused with the 60 kV of 28 MHz voltage. This reduced the peak current by ~ 25 %, substantially reducing fast losses that were limiting injection efficiency, resulting in a factor of two increase in the luminosity (Figs. 12 and 13). The RF defocusing also benefits the cooling efficiency. Ion focusing of the electron beam different is for different electron bunches, since the ion beam current varies longitudinally. This causes different space charge focusing of the electrons from bunch to bunch [24], increasing their angular spread and reducing the cooling efficiency. The region of flat ion current makes the effect of the ions on the electrons more uniform and thus easier to optimize on average.

CONCLUSIONS AND FUTURE WORK

The RHIC heavy ion and spin physics program requirement provide an array of intensity and space charge related challenges to performance optimization. Space charge driven bottlenecks in the injectors and mitigating efforts including bunch lengthening and stopband correction were described. The low-energy BES-II program in RHIC presented a unique combination of effects, not normally present

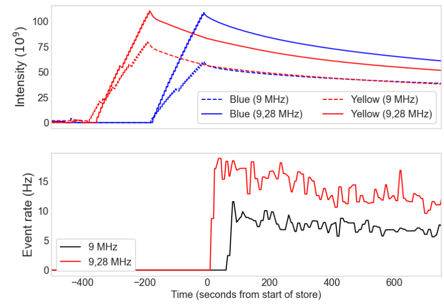

Figure 13: Intensity and luminosity comparison for two RHIC 3.85 GeV/n gold fills with and without bunch flattening using the 28 MHz RF. Intensity is shown for both the Blue and Yellow rings. Event rate is from the STAR detector. Extracted intensity from the AGS was the same in both cases.

in collider operation at the nominal high energies. Intensity dependent effects in the collider complex have largely been approached empirically on a case-by-case basis. In the future, more comprehensive simulations could be performed to identify specific drivers of intensity dependent emittance growth and beam loss.

REFERENCES

[1] C. Liu *et al.*, "Gold-gold luminosity increase in rhic for a beam energy scan with colliding beam energies extending below the nominal injection energy," *Phys. Rev. Accel. Beams*, vol. 25, no. 5, p. 051 001, 2022. doi:10.1103/PhysRevAccelBeams.25.051001

[2] M. Stephanov, K. Rajagopal, and E. Shuryak, "Signatures of the tricritical point in QCD," *Phys. Rev. Lett.*, vol. 81, no. 22, pp. 4816–4819, 1998. doi:10.1103/PhysRevLett.81.4816

[3] G. S. F. Stephans, "critRHIC: The RHIC low energy program," *J. Phys. G: Nucl. Part. Phys.*, vol. 32, no. 12, p. S447, 2006. doi:10.1088/0954-3899/32/12/S54

[4] E.-C. Aschenauer *et al.*, *The RHIC Cold QCD Program*, 2023.

[5] H. Huang *et al.*, "Acceleration of polarized protons in the ags with two helical partial snakes," in *Proc. PAC'05*, Knoxville, TN, USA, May 2005, pp. 1404–1406.

[6] W. Fischer and A. Bazilevsky, "Impact of three-dimensional polarization profiles on spin-dependent measurements in colliding beam experiments," *Phys. Rev. Spec. Top. Accel. Beams*, vol. 15, no. 4, p. 041 001, 2012. doi:10.1103/PhysRevSTAB.15.041001

[7] X. Gu *et al.*, "RHIC Au-Au operation at 100 GeV in Run16," in *Proc. NAPAC'16*, Chicago, IL, USA, Oct. 2016, pp. 42–44. doi:10.18429/JACoW-NAPAC2016-MOB3CO03

[8] S. Seletskiy *et al.*, "Accurate setting of electron energy for demonstration of first hadron beam cooling with rf-accelerated electron bunches," *Phys. Rev. Accel. Beams*, vol. 22, no. 11, p. 111 004, 2019. doi:10.1103/PhysRevAccelBeams.22.111004

[9] S. Seletskiy *et al.*, "Obtaining transverse cooling with non-magnetized electron beam," *Phys. Rev. Accel. Beams*, vol. 23, no. 11, p. 110 101, 2020. doi:10.1103/PhysRevAccelBeams.23.110101

[10] D. Kayran *et al.*, "High-brightness electron beams for linac-based bunched beam electron cooling," *Phys. Rev. Accel. Beams*, vol. 23, no. 2, p. 021 003, 2020. doi:10.1103/PhysRevAccelBeams.23.021003

[11] S. Lee, *Spin dynamics and snakes in synchrotrons*. World Scientific, 1997.

[12] K. Brown *et al.*, "Minimizing emittance growth during H^- injection in the ags Booster," Brookhaven National Laboratory, Upton, NY, USA, Tech Note BNL-81800-2009-CP, 2009.

[13] C. Liu *et al.*, "Rematching AGS Booster synchrotron injection lattice for smaller transverse beam emittances," in *Proc. IPAC'17*, Copenhagen, Denmark, May 2017, pp. 3353–3355. doi:10.18429/JACoW-IPAC2017-WEPVA041

[14] C. Gardner, "Simulation of turn-by-turn passage of protons through the H-minus stripping foil in Booster," Brookhaven National Laboratory, Upton, NY, USA, Tech Note C-A/AP/588, 2017.

[15] C. Gardner, "The Booster stopband correction system," Brookhaven National Laboratory, Upton, NY, USA, Tech Note AGS/AD/Tech Note No. 465, 1997.

[16] C. Gardner, Y. Shoji, L. Ahrens, J. Glenn, Y. Lee, and T. Roser, "Observation and Correction of Resonance Stopbands in the AGS Booster," in *Proc. PAC'93*, Washington D.C., USA, Mar. 1993, pp. 3633–3636.

[17] J. Brennan *et al.*, "High-intensity performance of the Brookhaven AGS," in *Proc. PAC'99*, New York, NY, USA, Mar. 1999, pp. 614–616. https://jacow.org/p99/papers/FRAR3.pdf

[18] K. Zeno, "An overview of Booster and AGS polarized proton operations during Run 17," Brookhaven National Laboratory, Upton, NY, USA, Tech Note BNL-81800-2009-CP, 2017.

[19] C. Gardner, "Booster double harmonic setup notes," Brookhaven National Laboratory, Upton, NY, USA, Tech Note C-A/AP/535, 2015.

[20] K. Zeno, "Overview and analysis of the 2016 gold run in the Booster and AGS," Brookhaven National Laboratory, Upton, NY, USA, Tech Note C-A/AP/571, 2016.

[21] C. Gardner, "Simulation of 6 to 3 to 1 merge and squeeze of Au77+ bunches in AGS," Brookhaven National Laboratory, Upton, NY, USA, Tech Note C-A/AP/563, 2016.

[22] J. Wei, A. Fedotov, W. Fischer, N. Malitsky, G. Parzen, and J. Qiang, "Intra-beam Scattering Theory and RHIC Experiments," *AIP Conference Proceedings*, vol. 773, no. 1, pp. 389–393, 2005. doi:10.1063/1.1949570

[23] S. Seletskiy, A. V. Fedotov, and D. Kayran, "Studies of ion beam heating by electron beams," in *Proc. NAPAC'22*, Albuquerque, NM, USA, Nov. 2022, pp. 343–346. doi:10.18429/JACoW-NAPAC2022-TUZE5

[24] H. Zhao *et al.*, "Cooling simulation and experimental benchmarking for an rf-based electron cooler," *Phys. Rev. Accel. Beams*, vol. 23, no. 7, p. 074 201, 2020. doi:10.1103/PhysRevAccelBeams.23.074201